REVISTA DCS
FUNDADA EN 2000

RHYACIAN/OROSIRIAN POST-COLLISIONAL POTASSIC ALKALINE MAGMATISM IN THE SÃO FRANCISCO CRATON- CERAÍMA MASSIF, SW OF THE STATE OF BAHIA, BRAZIL

MAGMATISMO ALCALINO POTÁSSICO PÓS-COLISIONAL RIACIANO/OROSIRIANO NO CRÁTON DE SÃO FRANCISCO - MACIÇO DE CERAÍMA, SUDOESTE DO ESTADO DA BAHIA, BRASIL

MAGMATISMO ALCALINO POST-COLISIONAL RIÁCICO/OROSIRIANO EN EL CRATON DE SÃO FRANCISCO - MACIZO DE CERAÍMA, SO DEL ESTADO DE BAHÍA, BRASIL

Joilma Prazeres Santos[1], Nilson Francisquini Botelho[2]

DOI: 10.54899/dcs.v23i86.4209
Recibido: 10/01/2026 | Aceptado: 13/01/2026 | Publicación en línea: 26/01/2026.

ABSTRACT

The Ceraíma Massif is located in the western sector of the State of Bahia, between the cities of Guanambi and Ceraíma, as part of the central-southern portion of the Gavião Block in the São Francisco Craton. Nearly-vertical, magmatic foliation shows a NS direction, discordant with the regional tectonic foliation. The Ceraíma Massif is made up of five petrographic facies: monzonite, quartz monzonite, porphyritic syenite, porphyritic syenite with mafic matrix and syenogranite. These facies characterize two magmatic affiliations; a monzonitic series and an alkaline silica-saturated series. The Ceraíma Massif can be arranged into two groups; syenitic and monzonitic, both metaluminous to slightly peraluminous, with syenogranite being the most evolved facies of the syenitic group. The geochemical signature also indicates that the facies of the Ceraíma Massif are cogenetic with each other as well as with the facies of the Guanambi Massif, demonstrating the occurrence of at least two magmatic pulses that originated from a single source of lithospheric mantle, metasomatized by influence of previous subduction processes.The age and geochemical features point to a post- collisional tectonic setting for the emplacement of the Ceraíma Massif magmas.

Keywords: Alkaline Potassic. Ultrapotassic. Shoshonite. Post-collisional.

RESUMO

O Maciço Ceraíma está localizado no setor oeste do Estado da Bahia, entre as cidades de Guanambi e Ceraíma, como parte da porção centro-sul do Bloco Gavião, no Cráton São Francisco. A foliação magmática, quase vertical, apresenta direção N-S, discordante com a foliação tectônica regional. O Maciço Ceraíma é composto por cinco fácies petrográficas: monzonito, monzonito quartzífero, sienito porfirítico, sienito porfirítico com matriz máfica e

[1] Doctor of Geology, Universidade de Brasília (UNB), Barreiras, Bahia, Brazil. E-mail: jpssantos@ufob.edu.br
[2] Doctor of Geology, Université Pierre et Marie Curie (LISE - CNRS), Brasília, Distrito Federal, Brazil.
E-mail: nilsonfb@unb.br

sienogranito. Essas fácies caracterizam duas afiliações magmáticas: uma série monzonítica e uma série alcalina saturada em sílica. A sequência de cristalização é marcada pela formação inicial de apatita, zircão e magnetita, seguida por diópsido, microclina e, mais recentemente, edenita, magnesiohornblenda e flogopita, com pequenas quantidades de anita e plagioclásio. O clinopiroxênio está ausente na fácies sienogranítica. Processos pós-magmáticos deram origem à clorita, actinolita e muscovita. O Maciço Ceraíma podem ser organizado em dois grupos: sienítico e monzonítico, ambos metaluminosos a ligeiramente peraluminosos, sendo o sienogranito a fácies mais evoluída do grupo sienítico. A assinatura geoquímica também indica que as fácies do Maciço Ceraíma são cogênicas entre si, bem como com as fácies do Maciço Guanambi, demonstrando a ocorrência de pelo menos dois pulsos magmáticos originados de uma única fonte de manto litosférico, metassomatizado pela influência de processos de subducção anteriores. A idade e as características geoquímicas apontam para um contexto tectônico pós-colisional para a intrusão dos magmas do Maciço Ceraíma.

Palavras-chave: Potássico Alcalino. Ultrapotássico. Shoshonita. Pós-colisional.

RESUMEN

El Macizo de Ceraíma se ubica en el sector occidental del Estado de Bahía, entre las ciudades de Guanambi y Ceraíma, como parte de la porción centro-sur del Bloque Gavião en el Cratón São Francisco. La foliación magmática, casi vertical, muestra una dirección NS, discordante con la foliación tectónica regional. El Macizo de Ceraíma está conformado por cinco facies petrográficas: monzonita, monzonita cuarzosa, sienita porfídica, sienita porfídica con matriz máfica y sienogranito. Estas facies caracterizan dos afiliaciones magmáticas: una serie monzonítica y una serie alcalina saturada de sílice. Los bloques del Macizo Ceraíma se pueden organizar en dos grupos: sienítico y monzonítico, ambos metaluminosos a ligeramente peraluminosos, siendo el sienogranito la facies más evolucionada del grupo sienítico. La firma geoquímica también indica que las facies del Macizo Ceraíma son cogenéticas entre sí, así como con las facies del Macizo Guanambi, lo que demuestra la ocurrencia de al menos dos pulsos magmáticos que se originaron a partir de una sola fuente de manto litosférico, metasomatizado por influencia de procesos de subducción previos. La edad y las características geoquímicas apuntan a un entorno tectónico postcolisión para el emplazamiento de los magmas del Macizo Ceraíma.

Palabras clave: Potásico Alcalino. Ultrapotásico. Shoshonita. Postcolisión.

INTRODUCTION

Potassic and ultrapotassic magmatisms commonly occur in volcanic and plutonic associations, in many cases related to minettes (Paim, 2014) sometimes referred to as lamproites (Foley et al.1987; Conceição et al., 1997a). Foley et al. (1987) defined high-potassium magmatism rocks having K_2O > 3 wt.%, MgO > 3 wt.% and K_2O/Na_2O > 2 for whole-rock analyses. However, Plá Cid et al (2000) considered that differentiated, intermediate acid rocks with MgO < 3 wt.% and $K_2O/Na_2O \approx 2$ should also be included within the ultrapotassic association. Even though some authors (e.g., Nardi et al. 2008) consider the relationship between alkaline-potassic and ultrapotassic magmatisms and the shoshonitic series a controversial issue, several authors (e.g., Lameyre and Bowden, 1982 and Plá Cid et al., 2000) relate alkaline high-potassium rocks to shoshonites.

Alkaline potassic and ultapotassic associations have been described by several authors from the Precambrian to the Cenozoic in different tectonic settings, mostly in ocean-island suites (Thompson and Fowler, 1986). However, post-collisional potassic and ultrapotassic syenitic rocks have also been reported by several authors (e.g., Thompson and Fowler, 1986; Nardi et al. 2008). Such rocks also constitute one of the most important syenitic provinces in the world, located in the northeastern and eastern sectors of Brazil, mainly in the state of Bahia (Conceição et al., 1997a, b; Rosa, 1999; Plá Cid et al., 2000; Paim, 2014). The Ceraíma Massif is part of this province, including several potassic to ultrapotassic intrusions located in the southwestern part of the state of Bahia. In the 1970s, the first description of alkaline rocks in southwestern Bahia was made during the Letos project (Barbosa and Moutinho, 1973), which grouped all magmatic occurrences in the region within the Guanambi Complex. Later, Leahy (1997), divided the Ceraíma Massif into three facies based on petrographic and geochemical data: porphyritic mafic syenites, trachytoids and granitic syenite. According to new field, petrographic and geochemistry data, Rosa (1999) reclassified the three facies previously described by Leahy (1997) with a zircon U-Pb age of 2.05 Ga, interpreting that the Ceraíma Massif originated within a post-collisional setting.

This paper presents new petrological, petrographic, and geochemical results that support the discussion on petrogenetic evolution, contributing to a better understanding of the crustal processes that gave rise to this vast Proterozoic alkaline magmatic province in the southwestern sector of the state of Bahia.

THEORETICAL FRAMEWORK

The Ceraíma massif is located in the south-central part of the São Francisco Craton, which corresponds to an internal and stable portion of a paleopeninsula of the São Francisco-Congo paleocontinent, one of the continents involved in the amalgamation of Western Gondwana. According to Barbosa et al. (2013) and Barbosa & Barbosa (2017), the Archean blocks (Gavião, Jequié and Serrinha) that constitute the São Francisco Craton were sutured along the Itabuna-Salvador-Curaçá belt.

Within this tectonic context, several Paleoproterozoic magmatic manifestations occur with pre, syn, late and post-collisional plutons emplaced in the Archean blocks. According to Guimarães (2005), pre-collisional, calcium-alkaline magmatisms were found at the margins of the Gavião and Serrinha blocks, of rhyacian age, with the Gavião block presenting ages between 2.3 and 2.1 Ga and the Serrinha block showing ages of approximately 2.1 Ga (Rios et al. 2000). Around 2.1 Ga (end of the rhyacian), the collision of the Gavião, Serrinha and Jequié blocks occurred, thus favoring the generation of syncollisional granitic magmatism (Rios et al. 2000). According to Rosa (1999) and Cruz et al. (2016), the emplacement of alkaline plutons, with ages between 1.9 and 2.05 Ga, occurred in the Western Gavião Block, after the collapse of the Itabuna-Salvador-Curaçá Belt. This collapse, according to Barbosa and Sabaté (2003), indicates that the region reached the peak of regional metamorphism around 2.0-2.1 Ga. More accurate geochronological data by Barbosa et al. (2017) and Martins de Sousa et al. (2020) reveal that the Itabuna-Salvador-Curaçá crustal segment reached the peak of regional metamorphism at approximately 2.09 to 2.1 Ga.

The research area is located in the south-central portion of the craton, specifically in the Western Gavião Block, which is composed of the Santa Isabel Complex, the Guanambi- Urandi Monzo-sienitic Batholith, the Espinhaço Supergroup and the recent covers.

Santa Isabel Complex

The Santa Isabel Complex crops out in the northern, eastern, southern, and southwestern portions of the study region, in the form of elongated hills and extensive cliffs, making tectonic contact with the Guanambi-Urandi Monzo-syenitic Batholith, and discontinuous with the Espinhaço Supergroup. The rocks that constitute the Santa Isabel Gneissic complex record ages of 3.18 to 2.95 Ga in the western portions of the Gavião block (Barbosa et al., 2013; Medeiros et al., 2017).

Guanambi-Urandi Monzo-Syenitic Batholith

The Guanambi-Urandi Monzo-syenitic Batholith (GUMSB), where is located the Ceraíma Massif, is a 6.000 km² terrain with 95% of outcropping rocks of syenitic to monzonitic composition (Rosa, 1999). The GUMSB is weakly deformed, with a smoothly sigmoidal feature and NW-SE magmatic foliation represented by oriented euhedral to slightly subhedral feldspars phenocrysts. All these features, further supported by lithogeochemical data, lead several authors (Rosa, 1999; Paim, 2014; Cruz et al., 2016) to suggest a post-collisional tectonic setting for emplacement of the GUMSB. However, Cruz et al. (2016) draw attention that trace elements signature, mainly Nb and Ta, suggests an association with an arc magmatic environment.

For Rosa (1999), this Paleoproterozoic magmatism presents two distinct domains: the multiple intrusions domain, which was subdivided into four facies (Paratinga, Laguna, Igaporã and Guanambi), and the late intrusions domain (Cara Suja, Ceraíma and Estreito massifs). In general, the domains are composed of rocks of predominantly leucocratic character, highlighting a varied composition from syenitic to monzonitic, with restricted monzodioritic to granitic terms and rare mafic enclaves.

The high potassium alkaline magmatism of southwestern Bahia has been dated by several authors, such as Mascarenhas & Garcia (1989) and Rosa (1999), who used the K-Ar, Rb-Sr, Pb-Pb and U-Pb methods and obtained ages between 2.0 and 2.05 Ga, interpreted as crystallization ages.

METHODOLOGY

The methods used in this research include fieldwork, petrography, mineral chemistry and whole-rock geochemistry.

- The field work was carried out over twenty-three days, with 70 points visited and 54 samples, giving rise to a 1.60.000 geological map.
- For the petrography, 32 thin sections were prepared at the thin section laboratory of the University of Brasília. Using the transmitted and reflected petrographic microscope, it was possible to determine the petrographic features.

Geochemical data were acquired for eighteen samples from the Ceraíma Massif (abbreviation Mc). The processing began with the crushing, quartering and grinding or spraying, leaving the rocks in the particle size fraction of 250 mesh, which were then sent for analysis at ACME Analytical Laboratories Ltd. Major and minor elements analysis were performed by inductively coupled plasma-atomic emission spectrometry (ICP-AES) and trace elements and rare earths (REE) were determined by inductively coupled plasma–mass spectrometry (ICP–MS). Nine analyses with acronyms of CMc were compiled from Leahy (1997), preserving the identification established by the author.

RESULTS AND DISCUSSION

Geology and Petrography of the Ceraíma Massif

The Ceraíma Massif corresponds to a zoned intrusion, in elliptical curved form, with facies structured in continuous layers, with NW-SE preferential direction (Figure 1). The contacts between the facies of the Ceraíma Massif are nearly sharp to gradational, while the contacts between the massif and the country rocks, Guanambi facies and Santa Isabel Complex, are tectonic. The rocks of the Ceraíma Massif are arranged in elevations ranging from 569 to 870m.

The rocks generally occur in the form of extensive slabs, rounded hills with a dome aspect, and ocassionally as loose blocks.

Figure 1. Geological map showing the five facies of the Ceraíma Massif.

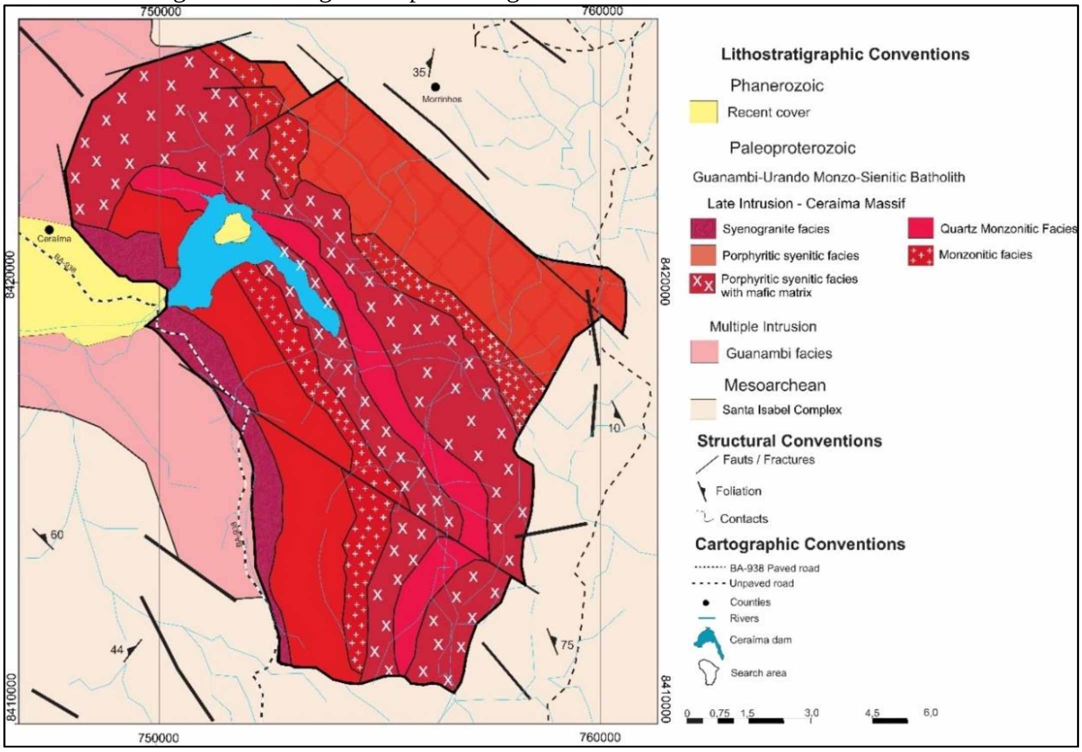

Source: Modified from Leahy (1997) and Rosa (1999).

Striking features in all facies of the massif consist of faults and narrow shear zones (Figure 3F) and fractures filled or not filled by hydrothermal alteration minerals, whose directions are between NW-SE and EW. The well-preserved magmatic foliation is marked by feldspar phenocrysts, which follow directions between N300° and 320°. The Ceraíma Massif was classified into five petrographic types: monzonite, quartz monzonite, porphyritic syenite, porphyritic syenite with a mafic matrix, and syenogranite (Figure 4). Using the parameters of the magmatic series proposed by Lameyre & Bowden (1982), the Ceraima Massif rocks show two smooth trends, towards the monzonitic-shoshonitic series and towards the alkaline silica-oversaturated series (Figure 4).

Porphyritic syenite

The porphyritic syenite presents gradational contact with the porphyritic syenite with mafic matrix and well-marked contact with the other facies of the massif. (Figure 1). The syenitic rocks are isotropic with restricted foliation marked by the orientation of the feldspars phenocrysts. It is pink in color due to the significant occurrence of euhedral to subhedral K-feldspar crystals, 10 to 15 mm long. K-feldspar phenocrysts are perthitic well-twinned microcline. Plagioclase grains are smaller than microcline, mineral is partialy altered by post-magmatic changes. Albite is generally found at the edge of oligoclase and in the interstices associated with biotite, hornblende, and quartz. The pyroxene grains (diopside and rare augite) are arranged interstitially or as agglomerates, with some edges filled with magnetite and amphibole (Figures 5B and C). Amphiboles are hornblende and actinolite. Hornblende, pleochroic to yellowish-green or brownish-green, forms prismatic crystals (Figure 2C). Fibrous actinolite, occurs filling the edges and planes of cleavage of hornblende and pyroxene. Biotite forms lamellae in the interstices between the feldspars, with a strong pleochroism from yellow to reddish brown.

Monzonite

The monzonite occurs in two strips located between the porphyritic syenite and the porphyritic syenite with mafic matrix (Figure 1). In general, the monzonite is dark gray, with greenish tones, isotropic with fine to medium grains (Figure 3I). No magmatic flow features were identified. K-feldspar is a perthitic microcline that ranges from small interstitial grains to 1 cm long subhedral crystals (Figure 2D). Plagioclase (oligoclase) forms subhedral fine grains, partialy replaced by albite at the edges and by muscovite and xenomorphic epidote at the core. Prismatic hornblende grains are arranged interstitially and are partially replaced by chlorite, titanite and magnetite at the edges and cleavage planes (Figure 2E). Biotite lamellae, occurs as intersticial agglomerates. Diopside, up to 1 mm in size, is rare and forms reaction rims at the edges of hornblende.

Porphyritic syenite with Mafic Matrix

The Porphyritic syenite is characterized by a fine to medium mafic matrix surrounding subhedral to euhedral K-feldspar and plagioclase phenocrysts (up to 3cm). The proportion of phenocrysts ranges from 20% to 40 %. The matrix is essentially constituted by hornblende, biotite, diopside/augite, quartz and magnetite. K-feldspar, the most abundant of the phenocrysts, occurs as tabular well-twinned microperthitic microcline crystal as long as 2 cm. Plagioclase phenocrysts is represented by prismatic oligoclase and albite, with dimensions up to 3 mm and partially altered by saussuritization and sericitization in the core (Figure 2F). Pyroxene occurs as 0.5 to 2 mm, hypidiomorphic to xenomorphic grains, with reaction rims with hornblende (Figure

2G). Hornblende forms poikilitic crystals (Figure 2H) and biotite occurs as clusters, both with inclusions of zircon and apatite.

Figure 2: (A) Microcline phenocrysts with films and spots of perthite, slightly altered to fine muscovite, in the porphyritic syenite. (B) Diopside with edges corroded by magnetite in the porphyritic syenite. (C) Growth of albite at the contact between perthitic microcline and oligoclase in the porphyritic syenite. (D) Microcline with Inclusion of apatite and albite in the monzonite. (E) Pyroxene, with diopside composition in the core and augite in the edge, in irregular contact with hypidiomorphic hornblende clusters, in the monzonite. (F) Oligoclase partially altered to white mica, quartz and epidote, with edges corroded by quartz, in the porphyritic syenite with mafic matrix. (G) Diopside aggregates with edges transformed into magnetite and hornblende in the porphyritic syenite with mafic matrix. (H) Poikilitic hornblende in the porphyritic syenite with a mafic matrix. (I) Sagenitic biotite, with edges corroded by chlorite and quartz, in the quartz monzonite. (J) Clusters of biotite altered to chlorite and muscovite in the quartz monzonite. (K) Intergrowth between quartz and plagioclase in contact with microcline, indicating a myrmekitic texture. (L) Titanite, biotite and intensely saussuritized oligoclase in the syenogranite.

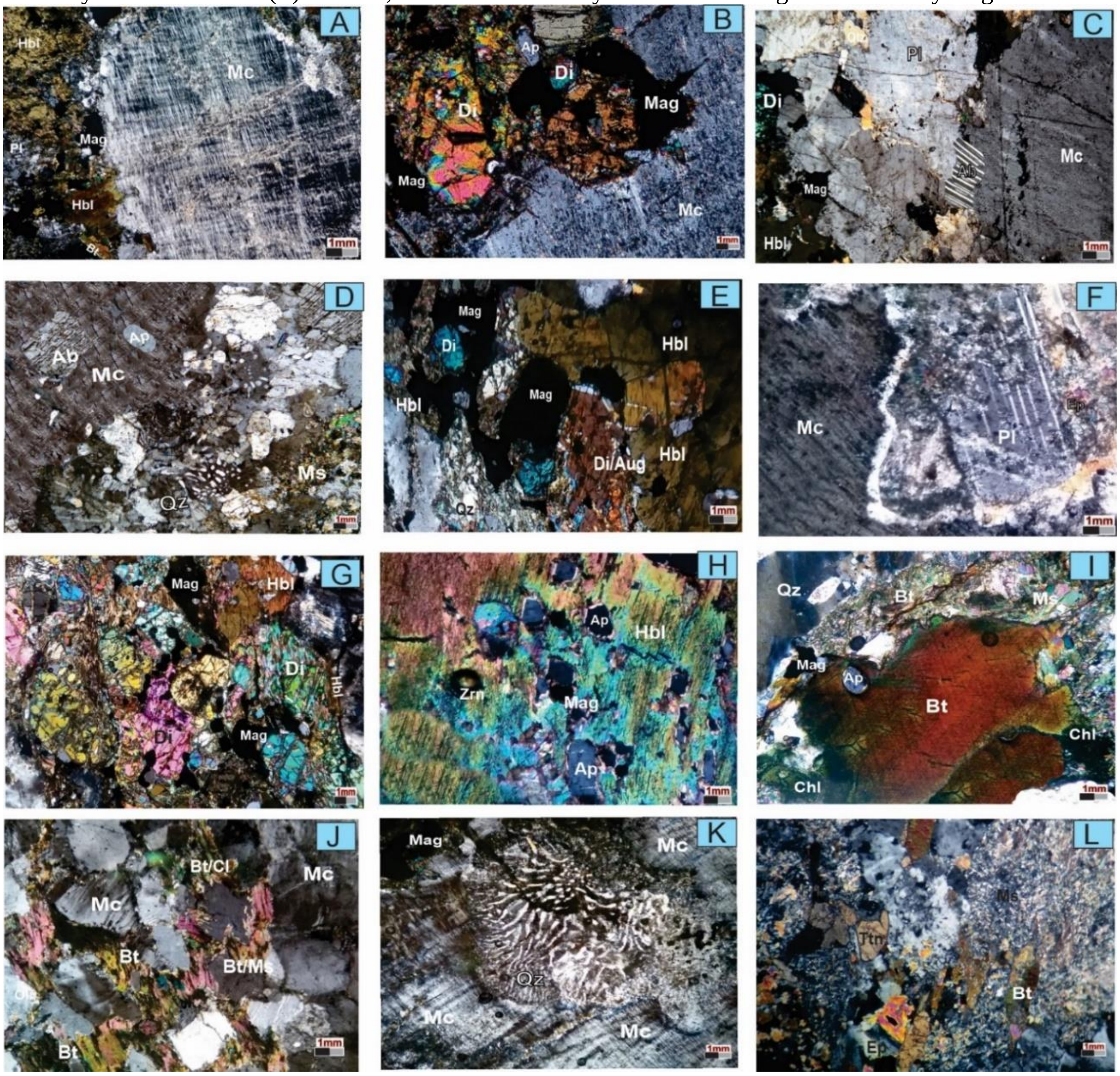

Source: Prepared by the authors themselves.

Quartz Monzonite

The quartz monzonite occurs only in the central sector of the massif as an elongated NW-SE. The quartz monzonitic rocks present a dark gray color tending to black, with some pinkish to whitish portions, and is fine to medium grained, with an equigranular to inequigranular texture and rare, phenocrysts of plagioclase and K-feldspar. Sericitization, suasuritization and chloritization are widespread in the quartz monzonitic rocks. Microcline occurs with inclusions of magnetite, apatite and zircon, and partially replaced by a mass of quartz, biotite, muscovite and epidote. Plagioclase occurs as intersticial grains, with composition ranging from albite to andesine (Figure 2I). The hornblende grains are replaced by chlorite, magnetite and titanite (Figure 2I). Biotite occurs as aggregates or isolated lamellae, with size ranging from 0.2 to 1.5 mm. The mineral is partially replaced by chlorite, magnetite and muscovite, and occasionally have inclusions of rutile needles, composing a sagenitic texture (Figures 5I and J). Diopside and augite have prismatic habit and reaction rims with hornblende.

Syenogranite

The syenogranite was mapped exclusively in the western border of the Massif area, where it is in tectonic contact with the Santa Isabel complex and Guanambi facies (Figure 1). . The sienogranitic rocks have medium- to coarse-grained inequigranular texture, with crystal shapes ranging from subhedral to anhedral. The essential minerals are microcline, oligoclase and quartz in addition to biotite and hornblende as randomly distributed mafic aggregates. Microcline exhibit dimension up to 10 mm, with a tartan type twinning, occasionally interrupted by perthite films and spots. Myrmekitic intergrowth is common at the contacts between microcline and plagioclase (Figure 2K). Oligoclase shows an intense alteration forming white mica and epidote masses (saussuritization, Figure 2L).

Lithogeochemistry

The purpose of the lithogeochemical study, in addition to the characterization of the rocks of the Ceraíma Massif, is their comparison with the rocks of the Guanambi facies, made up of of syenite, quartz syenite, quartz monzonite and granite (Figure 3A), whose data were compiled from Rosa (1999) and plotted together with the Ceraíma Massif data.

The Ceraíma Massif consists of syenites and monzonite of predominantly intermediate chemical composition (SiO_2 between 52.7 and 61.3%), with minor acid rocks (SiO_2 between 69.7 and 71.4%), represented by syenogranite (Table 1). According to the criteria established by Frost et al (2001), the studied rocks show two affinities, alkaline, represented by the syenites, and alkaline-calcic, which corresponds to the monzonite, quartz monzonite and syenogranite (Figure 3B). Thus, for the presentation of the lithogeochemical data, the porphyritic syenite and the porphyritic syenite with mafic matrix are called syenitic group, and the monzonite and quartz monzonite are called monzonitic group, all exhibiting magnesian signature (Figure 3 C), of shoshonitic to ultrapotassic nature (Figure 3D-E). According to Shand's alumina saturation index, the rocks of the Ceraíma Massif and the Guanambi facies are metaluminous to weaklly peraluminous in the syenogranites (Figure 3F).

For the analysis of the behavior of major and trace elements, we chose MgO, instead of SiO_2, as a differentiation index due to its wide variation (0.49 and 11.7%) in the studied rocks. The distribution of the major elements in binary diagrams indicates a clear definition of at least two distinct trends: one referring to the syenitic group and the other is expressed by the monzonitic group (quartz monzonite and monzonite).

Figure 3. Classification diagrams for the Ceraíma Massif rocks. A) Q-P of Debon & Le Fort (1983)-abr.: gr-granite; mzq-quartz monzonite; mz-monzonite; s-syenite, B) The alumina saturation index of Shand (in Maniar and Piccoli (1989), C) Na_2O+K_2O-CaO vs. SiO_2 demonstrating the compositional variation fields of the alkaline magmatic series according to Frost et al., (2001), D) $FeO_t/(FeO_t+MgO)$ versus SiO_2 by Frost et al. (2001), E) Diagram Th/Yb versus Ta/Yb proposed by Müller and Groves (1992) and F) K_2O vs. Na_2O marking the field of ultrapotassic, shoshonitic and calcium-alkaline rocks proposed by Turner et al. (1996). The gray circle symbol corresponds to the composition of the Guanambi Facies (compiled by Rosa, 1999).

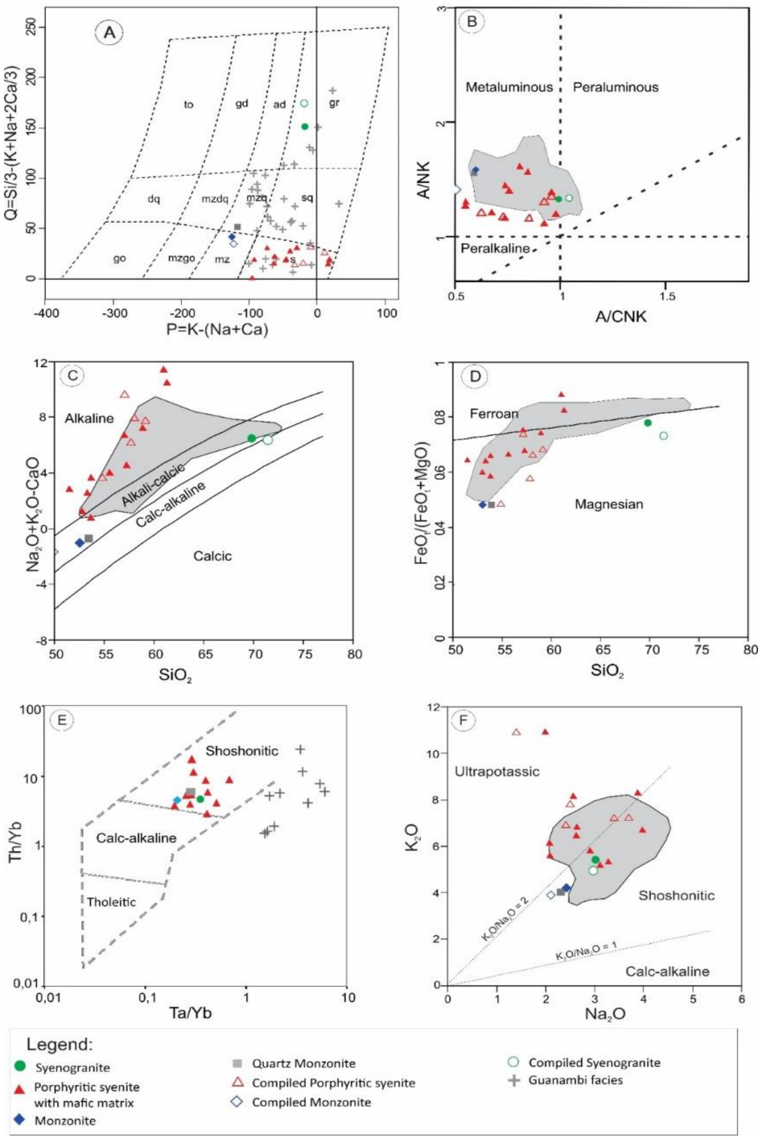

Source: Prepared by the authors themselves.

The binary diagrams show similarities between the geochemical signature of the Ceraima Massif and the Guanambi facies, highlighted by decreasing in TiO_2, CaO and P_2O_3, and increasing in Al_2O_3 and K_2O contents as the magmatic differentiation progresses. The higher amount of $Fe_2O_{3(t)}$ in the Ceraíma Massif comes from the porphyritic syenite with mafic matrix, absent or not sampled in the Guanambi facies. SiO_2 shows a normal negative correlation with CaO and CaO and MgO show a positive correlation, with higher levels in the monzonitic rocks and lower values in the syenogranitic facies.

The distribution of trace elements composition in the binary diagram reveals two trends, one represented by the syenitic group and the other trend corresponding to the monzonitic group. When comparing the Rb and Sr concentrations, it is possible to observe that the samples of the syenitic group are more enriched in these elements than those of the monzonitic group.

On the other hand, when analyzing the variation diagrams of the trace elements with slightly similar partition coefficients, the samples are arranged in clusters without a clear differentiation between them. The rocks of the Ceraíma Massif show Cs contents ranging from 0.68 to 3.86 ppm, with Rb/Cs ratios between 145 and 225, Y/Nb ratios between 1.2 and 4.4, and Nb/Ta ratios ranging from 17.36 to 27.71 except for three samples that indicated values of 7.79, 14.66 and 17.13.

The multi-elementary diagram, normalized for the primitive mantle according to Sun and McDonough (1989), shows a high content of LILE (Ba, Sr, K and Rb) and low content of HFSE (Nb, Ta, P, Ti). There is significant negative anomalies in Nb, P and Ti (Figure 4A), for both the Ceraíma Massif and for the Guanambi facies.

The patterns of rare earth elements normalized to the chondrite of Boynton (1984) show enrichment in light rare earth elements, when compared to the heavy rare earth elements (Figure 4B), with a $[La/Yb]_N$ ratio between 29.7 and 145.7. They present weakly negative to weakly positive anomalies in Eu (Figure 4B), with a $[Eu/Eu]_N$ ratio between 0.59 and 1.72 (Table 1). In the diagram Rb vs. (Y+Nb) proposed by Pearce (1996), the studied rocks and the Guanambi facies are plotted in the field of granitoids in a post-collisional environment (Figure 4C). Schandl & Gorton (2002) diagrams of Th/Ta vs. Yb (Figure 4 D) indicates an active continental margin for the analyzed rocks of the massif. Based on the P_2O_5/TiO_2 vs. TiO_2 (Foley et al., 1987) and Nb vs. Zr (Thompson and Fowler, 1986), the samples of the Ceraíma Massif and the Guanambi facies plot in the field of potassic rocks of an active continental margin (Figure 4D), except for the syenogranitic facies of the Ceraíma Massif, which were not reported in the diagram of Thompson and Fowler (1986) due to SiO_2 contents greater than 60%.

Table 1. Chemical analysis of the major elements, trace elements and rare earth elements of the Ceraíma Massif.

	FSPM e FSP										
Sample	MC 08	MC 15	MC 26 A	MC 28	MC 29	MC 30A	MC 33A	MC 34	MC 38	MC 39 A	MC 42 A
SiO_2	57.1	53	55.6	58.9	61.3	61	53.7	57.3	53.7	51.5	53.3
TiO_2	0.96	1.25	1.14	0.84	0.76	1.12	1.32	1.16	1.17	1.59	1.32
Al_2O_3	15	12.55	15.6	18.95	18.15	16.6	17.15	13.95	12.2	16	17.1
Fe_2O_3	7.81	8.75	7.76	4.36	3.84	4.57	7.46	7.43	8.61	8.69	7.8
MnO	0.12	0.15	0.12	0.07	0.06	0.08	0.12	0.13	0.14	0.12	0.14
MgO	2.33	5.31	3.55	1.35	0.75	0.57	3.54	3.23	5.52	4.33	3.94
CaO	4.06	7.03	5.12	3.32	1.76	1.57	5.1	4.95	6.95	5.77	5.74
Na_2O	2.57	2.08	2.62	3.98	3.88	1.99	2.91	2.64	2.09	3.28	3.1
K_2O	8.12	6.11	6.44	6.67	8.29	10.9	5.77	6.8	5.58	5.3	5.18
CO_2	n.a	n.a	n.a	n.a	n.a	n.a	n.a	n.a	n.a	n.a	n.a
H_2O^+	n.a	n.a	n.a	n.a	n.a	n.a	n.a	n.a	n.a	n.a	n.a
F	n.a	n.a	n.a	n.a	n.a	n.a	n.a	n.a	n.a	n.a	n.a
P_2O_5	0.83	1.29	0.88	0.36	0.17	0.12	0.77	1.03	1.22	1,0	0.73
LOI	0.65	0.97	1.25	1.45	1.02	0.52	1.61	0.68	1.55	1.02	1.63
Total	99.55	98.49	100.08	100.25	99.98	99.04	99.45	99.3	98.73	98.6	99.98
$Na_2O + K_2O$	10.69	8.19	9.06	10.65	12.17	12.89	8.68	9.44	7.67	8.58	8.28
K_2O/Na_2O	3.16	2.94	2.46	1.68	2.14	5.48	1.98	2.58	2.67	1.62	1.67
Rb	215	178.5	177	151	224	205	166	212	160	145	158
Ba	6690	4450	3960	4260	2700	324	2970	4310	4060	3830	2800
Nb	12.9	11.6	25.7	11.7	17.6	26.5	15.3	19.1	11.2	18.6	13.3
Sr	3530	1685	1625	1770	1175	2420	1260	2000	1260	2130	1295
Zr	411	343	673	665	1265	3220	558	461	230	131	642
Y	52.8	35	33.1	24	53.5	113	27.8	43.7	37.3	32.4	34.3
Ta	0.9	0.6	1.5	0.5	1.2	3.4	0.8	1.1	0.5	0.7	0.6
Hf	9.1	8.3	15.3	14	27.2	59.9	12.6	11.3	5.8	3.3	13.7
Th	17.55	12.9	20.2	31	47.1	28.3	11.65	25	10.15	5.17	8.97
Cs	2	2.67	1.88	0.68	0.74	0.87	1.48	2.67	1.85	1.09	1.2
Ga	22	19.4	23.7	25.4	25.1	22.6	23.5	22.2	22.9	25.9	24.2
La	249	169.5	183	292	372	393	169	217	148	188.5	189
Ce	523	352	373	558	839	793	325	437	306	369	345
Pr	65.9	42.6	44.5	57.4	80.9	121.5	37.7	53.2	37	44.9	42.3
Nd	244	153	151	190	273	442	129	189	143.5	157.5	148.5
Sm	39.5	25.7	24.6	24.2	38.3	76.4	19.45	30.5	25.6	24.4	22.4
Eu	8.16	5.64	6.03	6.09	7.95	15.85	5.03	6.59	5.09	6.25	5.82
Gd	26.7	16	14.45	13.05	22.4	48.5	11.9	18.45	16	14.8	13.4
Tb	2.79	1.83	1.67	1.16	2.62	5.85	1.3	2.07	1.88	1.73	1.63
Dy	12.45	8.13	7.6	5.58	12.1	26	6.25	9.57	8.18	7.6	6.94
Ho	2.07	1.2	1.16	0.93	2.04	4.05	1.02	1.44	1.28	1.18	1.16
Er	4.53	3.07	2.92	2.26	4.79	9.65	2.48	3.29	3.14	2.72	2.87
Tm	0.58	0.37	0.35	0.3	0.66	1.22	0.35	0.48	0.42	0.38	0.37
Yb	3.16	2.39	2.2	1.76	4.03	6.72	1.93	2.79	2.58	1.73	2.19
Lu	0.39	0.3	0.3	0.26	0.52	0.92	0.3	0.39	0.35	0.24	0.3
$(Eu/Eu^*)_N$	0.77	0.85	0.98	1.05	0.83	0.8	1.01	0.85	0.77	1.01	1.03
$(La/Yb)_N$	53.12	47.81	56.08	111.85	62.23	39.43	59.04	52.44	38.67	73.46	58.18

n.a - not analyzed

Source: Prepared by the authors themselves.

Figure 4. Multi-elementary and tectonic discrimination geochemical diagrams for the Ceraíma Massif rocks: A) Multi-elementary diagram normalized to the primitive mantle according to Sun and McDonough (1989); B) Rare earth elements normalized to the chondrite according to Boynton (1984); C) Rb versus Y + Nb proposed by Pearce et al. (1984) with the postcollisional granitoid field according to Pearce (1996) and D) Yb x Th/Ta diagram from Schandl & Gorton (2002). The gray field corresponds to the composition of the multiple intrusions of the Guanambi facies

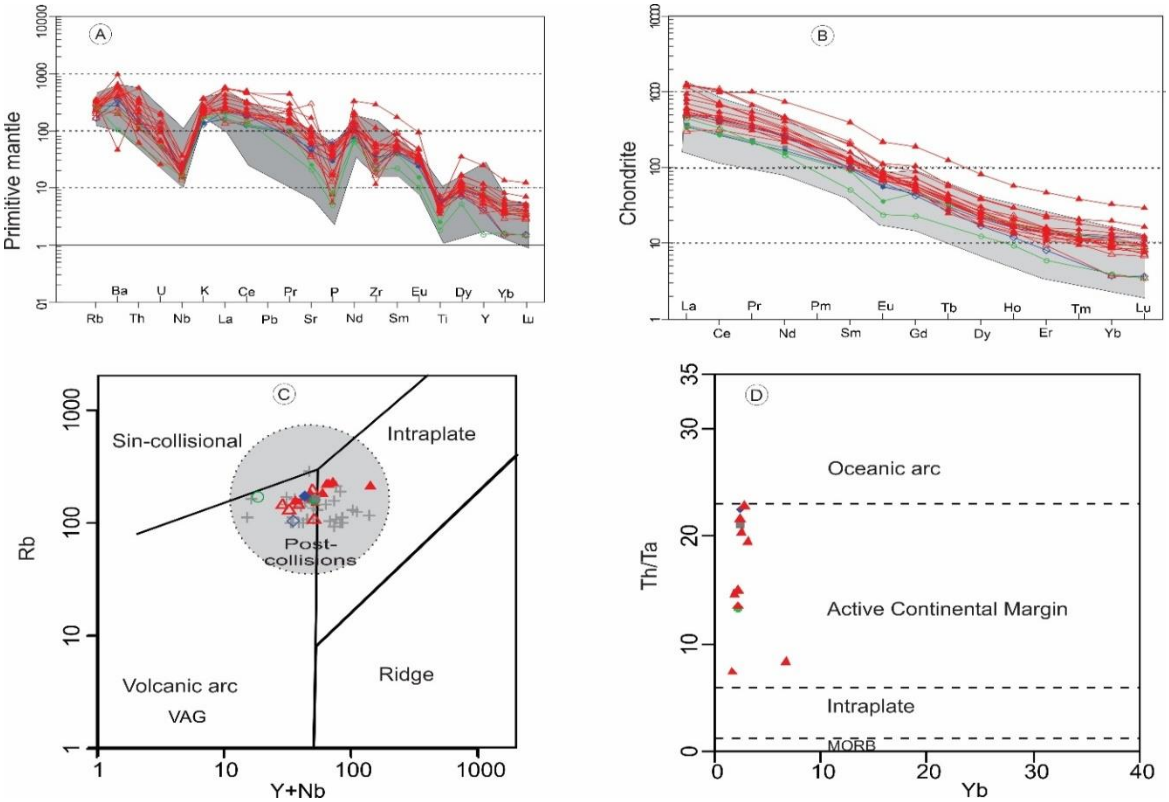

Source: (compiled from Rosa, 1999).

Geochemistry, Geochronology and Tectonic Setting

According to the Shand alumina saturation index, the rocks of the Ceraíma Massif are metaluminous with a slightly peraluminous character in the the syenogranitic facies. The association of diopside, edenite and epidote, highlighted by the enrichment in CaO, and A/CNK <1, demonstrates the metaluminous character of the Ceraíma Massif, However, the syenogranite, with a weak peraluminous tendency, have biotite in their modal composition, low CaO levels and A/CNK >1. According to Frost et al. (2001), rocks with a slightly peraluminous character have biotite as a probable phase to house excess Al, which cannot be accommodated in the feldspar structure. The major and trace elements present linear trends, indicating that the Ceraíma Massif expresses similarity with the Guanambi facies and can be divided into two groups, syenitic and monzonitic. In the case of Fe_2O_3, there is a change in the trend behavior, as the syenitic group and the syenogranitic facies express a positive correlation, while the monzonitic group shows an increase in concentrations during crystallization, thus reflecting the important role played by ferromagnesian minerals.

The high amounts of alkalis ($Na_2O + K_2O$), between 6.4 and 11.15%, the content of Al_2O_3, between 11.8 and 18.95%, and that of TiO_2, between 0, 4 and 1.3%, are within the parameters established by Morrison (1980) to classify the shoshonitic series. However, several samples have ratios of K_2O/Na_2O> 2, MgO> 3 and K_2O> 3, which, according to Foley et al. (1987), can be classified as ultrapotassic rocks.

These characteristics, together with the geochemical data that indicates high concentrations of LILEs and LREE in relation to the low levels of HFSE and HREE, suggest that the Ceraíma Massif rocks originated in a post-collisional environment affected by subduction processes, as proposed by Rosa (1999) and confirmed by the diagrams Yb versus Th/Ta of Schandl & Gorton (2002), P_2O_5/TiO_2 versus TiO_2 according to Foley et al. (1987) and Nb versus Zr proposed by Thompson and Fowler (1986), where the rocks of the Ceraíma Massif plot in the field of post-collisional rocks of active continental margin.The post-collisional rocks of the Shoshonitic Association of Lavras do Sul (Liz et al. 2009) and other rocks of shoshonitic signature, such as the Anuri Massif, Santanápolis and Cara Suja, in the state of Bahia, have characteristics similar to those observed in the Ceraíma Massif.

CONCLUSION

Based on the results, it is concluded that the Ceraíma Massif is composed of intermediate to acidic rocks, organized into five facies distributed with compositional contacts and belonging to the shoshonitic and monzonitic series. Petrographic and geochemical characterization allowed the recognition of a magmatic evolution in multiple stages of crystallization, from early phases to late- and post-magmatic processes. The massif presents an alkaline potassic geochemical signature of shoshonitic affinity, with ultrapotassic terms and a predominantly metaluminous character. Petrogenetic evolution indicates the existence of two lithological groups, with syenogranite being the most evolved term, generated mainly by fractional crystallization, possibly associated with more than one magmatic pulse from a common lithospheric source. Field, geochemical, and geochronological data suggest that the Ceraíma Massif was emplaced in a post-collisional tectonic context, with previous influence of subduction and mantle metasomatism in the São Francisco Craton.

ACKNOWLEDGMENTS

This study was supported by CAPES (Funding Code 001) and through a partnership between UFOB and UnB in the DINTER program, which provided infrastructure and resources. The authors thank the professors and collaborators who contributed geochemical data, field support, and fundamental scientific discussions to the development of the research.

REFERENCES

Barbosa J.S.F. & Barbosa R.G. The Paleoproterozoic eastern Bahia orogenic domain. In: Heilbron M., Cordani U. G., Alkmim F. F. (ed) São Francisco Craton, eastern Brazil (tectonic genealogy of a miniature continent). Rio de Janeiro, **Springer**, 57-69, 2017.

Barbosa N. S.; Teixeira W.; Bastos Leal L. R.; Leal A. B. M. Evolução crustal do setor ocidental do Bloco arqueano Gavião, cráton do São Francisco, com base em evidências U-Pb, Sm-Nd e Rb-Sr. **Geologia USP**, Série cientifica, 13(4), 6-88, 2013.

Barbosa, J.S.F.; Sabate, P., Marinho, M.M. O Cráton do São Francisco na Bahia, uma síntese. **Revista Brasileira de Geociências**. 33:3-6, 2003.

Barbosa, O. & Moutinho, Da Costa L.A. Projeto Leste de Tocantins - Oeste do Rio São Francisco (Letos), 2a etapa de campo, fase IV. **DNPM/CPRM/PROSPEC**, Rio de Janeiro-RJ, 8, 1973.

Boynton, W.V. Cosmochemistry of the rare earth elements: meteorite studies. In: Henderson P. (ed), Rare Earth Element Geochemistry, **Elsevier**, Amsterdam, 2, 63-114, 1984.

Conceição; H.; Oliveira; O.M.C.; Martin; H.; Rosa; M.L.S.; Conceição; R.V.; Plá Cid, J.. Petrologia do magmatismo alcalino potássico com afinidade lamprofírica e assinatura de subducção no sul do Estado da Bahia: Maciço Sienítico de Anuri. **Geochimica Brasiiensis**, 11(2), 171-186, 1997a.

Conceição, R.V.; Conceição, H.; Lafron, J.M. Petrologia dos sienitos alcalinos potássicos do Maciço Santanápolis, Ba, Geochimica Brasiliensis. 11, 133-152, 1997b.

Cruz; S.C.P.; Barbosa; J.S.F.; Pinto; M.S.; Peucat; J.J.; Paquette; J.L.; Souza; J.S.; Martins; V.S.; Chemale; Jr. F.; Carneiro, M.A. The Siderian-Orosirian magmatism in the Archean Gavião Paleoplate, Brazil: U-Pb geochronology, geochemistry and tectonic implications. **Journal South America**. Earth Sci., 69, 43-79, 2016.

Debon, F. & Le Fort, P. A chemical-mineralogical classification of common plutonic rocks and associations. **Transactions of the Royal Society of Edinburgh**. Ed.: Earth Sci., 73, 135-149, 1983.

Foley, S;F;, Venturelli, G;, Green, D;H;, Toscani, L. The ultrapotassic rocks: characteristics, classification and constrains for petrogenetic models. **Earth Science Reviews**, 24(2). 81- 134, 1987.

Frost, B;R;, Arculus, R;J;, Barnes, C;G;, Collins, W;J;, Ellis, D;J; & Frost, C.D. A geochemical classification of granitic rocks. **Journal of Petrology**, 42(11), 2033-2048, 2001.

Guimarães, J. T. **Projeto Ibitiara-Rio de Contas**, Estado da Bahia, Escala 1:200.000. Serviço Geologico do Brasil, CPRM, p. 217, 2005.

Lameyre, J.; Bowden, P. Plutonic rock type series: discrimination of various granitoid series and related rocks. **Journal of Volcanology and Geothermal Research**, 14, 169-186, 1982.

Leahy, G.A.S. **Caracterização Petrográfica e Litoquímica da Intrusão Sienítica de Ceraíma (Sudoeste da Bahia)**. 1997. MS Dissertation, Instituto de Geociências, Universidade Federal da Bahia. Salvador, 1997.

Liz, J;D;, Lima, E;F;, Nardi, L;V;S;, Sommer, C;A;, Saldanha, D;L;, Pierosan, R. Petrologia e sucessão estratigráfica das rochas monzoníticas da associação shoshonítica de Lavras do Sul (RS). **Revista Brasileira de Geociências**, 39, 244-255, 2009..

Maniar, P.D. & Piccoli, A. Tectonic Discrimination on Granitoids. **Geological Society of America Bulletin**, 101, 635-643, 1989.

Martins de Sousa, D;F;, Oliveira, E;P;, Amaral, W;S;, Baldim, M.R. The Itabuna-Salvador-Curaçá Orogen revisited, São Francisco Craton, Brazil: New zircon U–Pb ages and Hf data support evolution from archean continental arc to paleoproterozoic crustal reworking during block collision. **J. S. Am. Earth Sci**. 104, 2020.

Mascarenhas, J.F. & Garcia, T.W. **Mapa Geocronológico do Estado da Bahia**: texto explicativo. Superintendência de Geologia e Recursos Minerais, Sec. Minas e Energia, p. 189, 1989.

Medeiros E;L;M;, Cruz S; C; P;, Barbosa J;S;F;, Paquette J;L;, Peucat J;J;, Jesus S;S;G;P;, Barbosa R;G; Brito R;S;C;, Carneiro M.A. The Santa Izabel Complex, Gavião Block, Brazil: Components, geocronology, regional correlations and tectonic implications. **Journal of South American Earth Sciences**, 80, 66-94, 2017.

Morrison, G.W. Characteristics and tectonic setting of the shoshonite rock association. **Lithos**, 13(1), 98-108, 1980.

Muller, D.; Groves, D.I. Direct and indirect associations between potassic igneous rocks, shoshonites and gold-copper deposits. **Ore Geol. Rev**. 8, 383-406, 1993.

Nardi, L;V;S;, Plá Cid, J;, Bitencourt M;F;, Stabel, L. Geochemistry and petrogenesis of post-collisional ultrapotassic syenites and granites from southernmost Brazil: the Piquiri Syenite Massif. An. **Acad. bras. Ci**., 80 (2), 353-371, 2008.

Paim, M.M. 2014. **Maciço de Cara Suja: Expressão do Magmatismo Alcalino Potássico Pós-colisional no Sudoeste da Bahia**. PhD Thesis. Instituto de Geociências, Universidade Federal da Bahia. Salvador, p. 258, 2014.

Pearce, J. **Sources and settings of granitic rocks**. Episodes, 19(4), 120-125, 1996.

Pearce, J.A., Harris, N.B.W., Tindle, A.G. 1984. Trace element discrimination diagrams for the tectonic interpretation of granitic rocks. **Journal of Petrology**, 25, 956-983.

Plá Cid, P;J;, Nardi, L;V;S;, Conceição, H;, Bonin, B;, Jardim de Sá, E. The alkaline silica-saturated ultrapotassic magmatism of the Riacho do Pontal Fold Belt, NE Brazil: an example of syenite-granite Neoproterozoic association. J South Am Earth Sci 13, 661–683, 2000.

Rios, C; D;; Davis D; W;; Conceição, H;; Macambira, M; J; B;; Peixoto, A; A;; Cruz Filho, B;

E; da, Oliveira L. L. Ages of granites of the Serrinha nucleus, Bahia (Brazil): an

overview. **Revista Brasileira de Geociências**, 30, 74‑77, 2000.

Rosa, M.L.S. **Geologia geocronologia mineralogia litogeoquímica e petrologia do Batólito Monzo-Sienítico Guanambi-Urandi (SW-Bahia)**. 1999. PhD Thesis. Instituto de Geociências, Universidade Federal da Bahia. Salvador, 1999.

Schandl E.S.; Gorton M.P. Application of high field strength elements to discriminate tectonic settings in VMS environments. Economic Geology, 97, 629-642, 2002.

Streckeisen, A. To each plutonic rock its proper name. **Earth Science Reviews**, 12(1), 1-33, 1976.

Sun, S.S. and McDonough, W.F. Chemical and isotopic systematics of oceanic basalts, implications for mantle composition and processes. In: Magmatism in the ocean basins. Saunders, A.D. and Norry, M.J. (Editors), **Geological Society of London**, London, 42, 313-345, 1989.

Thompson, R.N. & Fowler, M.B. Subduction-related shoshonitic and ultrapotassic magmatism: a study of Siluro-Ordovician syenites from Scottish Caledonites. Contrib. **Mineral. Petrol.**, 14, 507-522, 1986.

Turner, S;, Arnaud, N;, Liu, J;, Rogers, N;, Hawkesworth, C;, Harris, N;, Kelley, S;, van Calsteren, P. & Deng, W. (1996). Post-collision, shoshonitic volcanism on the Tibetan Plateau: implications for convective thinning of the lithosphere and the source of ocean island basalts. Journal of Petrology 37, 45-71.